# Temperature dependence of Heteroeptaxial $Y_2O_3$ films grown on Si by ionized cluster beam deposition

M. -H. Cho, D. -H. Ko[1], S. W. Whangbo, H. B. Kim, K.H.Jeong, and C. N. Whang*

Atomic-scale Surface Science Research Center & Department of Physics, Yonsei University, Seoul 120-749, Korea

1 Department of Ceramic Engineering, Yonsei University, Seoul 120-749, Korea

S. C. Choi

Thin Film Science & Technology Center, Korea Institute of Science and Technology, Seoul 130-650, Korea

S. J. Cho

Department of Physics, Kyungseong University, Pusan 608-736, Korea

ABSTRACT

Heteroepitaxial $Y_2O_3$ films were grown on a Si(111) substrate by ionized cluster beam deposition (ICBD) in ultra high vacuum, and its qualities such as crystllitnity, film stress, and morphological characteristics were investigated using the various measurement methods. The crystallinity was investigated by x-ray diffraction (XRD) and reflection high energy electron diffraction (RHEED). Interface crystallinity was also examined by Rutherford backscattering spectroscopy (RBS) channeling, transmission electron microscopy (TEM). The stress of the

* corresponding author, fax: 82-2-312-7090, e-mail: cnwhang@bubble.yonsei.ac.kr

films was measured by RBS channeling and XRD. Surface and interface morphological characteristics were investigated by atomic force microscopy (AFM) and x-ray scattering method. Comparing the interface with the surface characteristics, we can conclude that many defects at the interface region were generated by interface reaction between the yttrium metal and $SiO_2$ layer and by ion beam characteristic such as shallow implantation, so that they influenced the film qualities. The film quality was dominantly depended on the characteristic temperature range. In the temperature range from 500 ℃ to 600 ℃, the crystallinity was mainly improved and the surface roughness was drastically decreased. On the other hand, in the temperature range from 600 ℃ to 700 ℃, the compressive stress and film density were dominantly increased, and the island size was more decreased. Also, the surface morphological shape was transformed from elliptical shape to triangular. The film stress existed dominantly at the interface region due to the defects generation.

## I. INTRODUCTION

Recently, studies on epitaxial growth have been carried out in yttira-stabilized zirconia(YSZ), $ZrO_2$, $CeO_2$, $PrO_2$ and $Y_2O_3$ [1-6]. The epitaxial films of these fluorite type oxide on Si are attractive materials for potential application in making highly integrated circuits as an alternative $SiO_2$ layer and for use in superconductor with high critical current density as buffer layers between oxide superconductor and Si. Especially, $Y_2O_3$ has a cubic $Mn_2O_3$ structure with a well-matched lattice parameter of 10.60 Å to Si (as compared to 5.43 Å for Si) and has a good chemical stability with a high melting point 2350 ℃. $Y_2O_3$ is also an interesting material with a high dielectric constant of about 13-17, which is desirable for a storage capacitor in the dynamic access memory [7-9]. These advantages enable the $Y_2O_3$ film to be used as a buffer layer for growing epitaxial superconducting film Ba-Y-Cu-O exhibiting high transition temperature and high critical current densities [10-11].

Although the $Y_2O_3$ film has many advantages in the applications, the studies on the physical properties such as the crystallinity, strain and surface morphology has not been deeply carried out [12-18]. In particular, the interface characteristic of the film related with growth and reaction at initial stage is important, because the film qualities depend on the interfacial bonding of the film to each other and to the substrate which causes physical and chemical interaction. That is, the films and substrate can be held under a state of compressive or tensile stress with each other by transmitting forces across the interfaces, and the crystallinity and the stress are affected by the interfacial bonding at initial growth stage. The crystallinity and the stress of the film are important for the application to buffer or dielectric insulator, because they often present detrimental effect on various properties of the film, in particular, thermal and mechanical stability, and adhesion. Moreover, the electrical properties can be affected by the crystallitnity, strain, and interface characteristics. Therefore, it is expected that this study will present the basic data for the application.

We have already reported the epitaxial growth of $Y_2O_3$ films on Si(100) substrate, which was characterized by reflection of high energy electron diffraction (RHEED), transmission electron microscopy (TEM) [19]. The TEM image shows the sharp distinction between film and substrate without any inter-layer oxide. We conjectured that this interface characteristic would be owing to the chemical reacton between yttrium and substrate.

Using ionized cluster beam deposition, the formation of silicon oxide at the interface was suppressed. The reaction mechanism at the interface has not been illustrated sufficiently yet. Through the various investigation, we studied the temperature dependence on the crystallinity, strain, and surface morphology of the heteroepitaxial $Y_2O_3$ film grown on Si substrate. We expect that the film characteristics depending on the substrate temperature will also present the information on the interface reaction.

In this study, the film properties such as the crystallinity, strain, and morphology were examined using RHEED, x-ray scattering, RBS channeling, TEM, and AFM. The $Y_2O_3$ films grown on Si(111) by ICB showed single crystalline structure over the substrate temperature of 500 ℃. Therefore, In the temperature range above the 500 ℃, the characteristics of the heteroepitaxial $Y_2O_3$ film on Si(111) such as crystallintiy, stress, and surface and interface morphology were investigated and discussed. In the temperature range from 500 ℃ to 600 ℃, the crystallinity was mainly improved and the surface roughness was drastically decreased. On the other hand, in the temperature range from 600 ℃ to 700 ℃, the compressive stress and film density were dominantly increased, and the island size was more decreased. Also, the surface morphological shape was transformed from elliptical shape to triangular. The crystallinity and the roughness at the interface region was worse than that at the surface region, so that the film stress existed dominantly at the interface region.

## II. EXPERIMENTS

$Y_2O_3$ films were deposited on a heated Si (111) substrate by ionized cluster beam of yttrium in ultra high vacuum. The base pressure of the growth chamber was below $5 \times 10^{-10}$ Torr, and the oxygen partial pressure was about $1 \times 10^{-5}$ Torr during the $Y_2O_3$ deposition. The substrate was heated by the electron beam method with a tungsten filament, and the temperature was monitored with an optical pyrometer. The Si substrate was a 4° vicinal (111) oriented single crystal wafer. The Si wafer was chemically cleaned and etched by diluted HF acid to remove the native oxide from the Si surface before being inserted into the chamber. The sample was transferred into UHV chamber via load lock system, and heated up to 1000 ℃ by e-beam bombardment until the clean $7 \times 7$ structure of the Si(111) surface was observed by RHEED. The deposition rate of

yttrium was controlled with about 0.3 Å/sec and the acceleration voltage of the yttrium ion cluster beam Vacc=5 kV, the electron gun bias Ve=400 V, and the electron beam current Ie=200 mA in the ionization region were fixed as an optimum ICB condition [20-22].

The dependence on the substrate temperature was investigated in the temperature of 500 ℃, 600 ℃, and 700 ℃. The crystallographic properties of $Y_2O_3$ film were investigated by XRD with Cu K $\alpha$ radiation and RHEED at acceleration beam energy of 30 keV. The surface morphology and interface were studied by AFM and x-ray scattering, respectively. RBS channeling, and XRD were used to ascertain the stress and the crystalline characteristic of $Y_2O_3$ film along the film depth direction. In the measurement of the RBS channeling, the detector angle is 170° with respect to the direction of the 2 MeV $He^{++}$ incident and nominal detector energy resolution is 14 keV. In order to investigate the crystallinity along the depth direction, the aligned spectra of interface and surface region were extracted respectively. The epitaxial growth and the interface characteristics of the film were also investigated by TEM.

## III. RESULTS and DICUSSION

### A. Crystallinity

We investigated the surface crystallinity of the films through the *in situ* RHEED observation. Figure 1 showed the RHEED patterns of $Y_2O_3$ films with the substrate temperature. The streak-like patterns indicated that the films had single crystalline structure with flat surface morphology. The substreak owing to the $Y_2O_3$ film surface unit cell structure which has four unit cells of $CaF_2$ structure was not observed below the substrate temperature of 600 ℃. The substreak became gradually clear as the substrate temperature increased up to 700 ℃. The variation of the streak length and width resulted from the film surface

crystallinity and surface roughness. The streak length became longer and the width narrower as the substrate temperature increased. This indicated that the crystallinity of the film surface was improved and the surface roughness was decreased as the substrate temperature increased. Especially, the appearance of the substreak pattern and the narrowing the streak width indicated that the improvement of the crystallinity between the substrate temperature of 500 ℃ and 600 ℃ was much more dominant than that of between the 600 ℃ and 700 ℃. The diffraction of the film had three fold symmetry and the width between the two main streak was approximately equal to the Si (111) plane in the incident beam direction along the Si [110]. Rotating the sample from the [110] direction to 30 ° along the Si [111] direction, the streak pattern showed the same diffraction as FCC structure in [112] direction. Moreover, for the whole range of deposition temperature employed, all the $Y_2O_3$ films were found to be (111) oriented by XRD, exhibiting only to (222) and (444) XRD reflections. Therefore, the growing direction relationship is as follows:

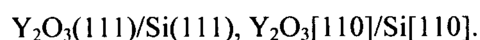
$Y_2O_3(111)/Si(111)$, $Y_2O_3[110]/Si[110]$.

The crystallinity of the film was also investigated by the RBS channeling. This method is useful for measuring the crystallinity and the stoichiometry of the film along the growth direction, whereas the RHEED observation can present the inspection of the crystallinity on the film surface. The minimum channeling yield (Xmin) indicated the change of crystallinity with the substrate temperature. Figure 2 showed the channeling spectra of the $Y_2O_3$ films at the substrate temperature of 500 ℃, 600 ℃, and 700 ℃. At the substrate temperature of 500 ℃, the channeling yield, 0.92, indicated that the alignment of the yttrium atoms in the $Y_2O_3$ film deviated from the channel path, which illustrated that the migration energy of the yttrium atoms was not fully supplied by the thermal energy of the substrate temperature 500 ℃. Increasing the substrate temperature up to 600 ℃, the channeling yield was drastically decreased to 0.26 at

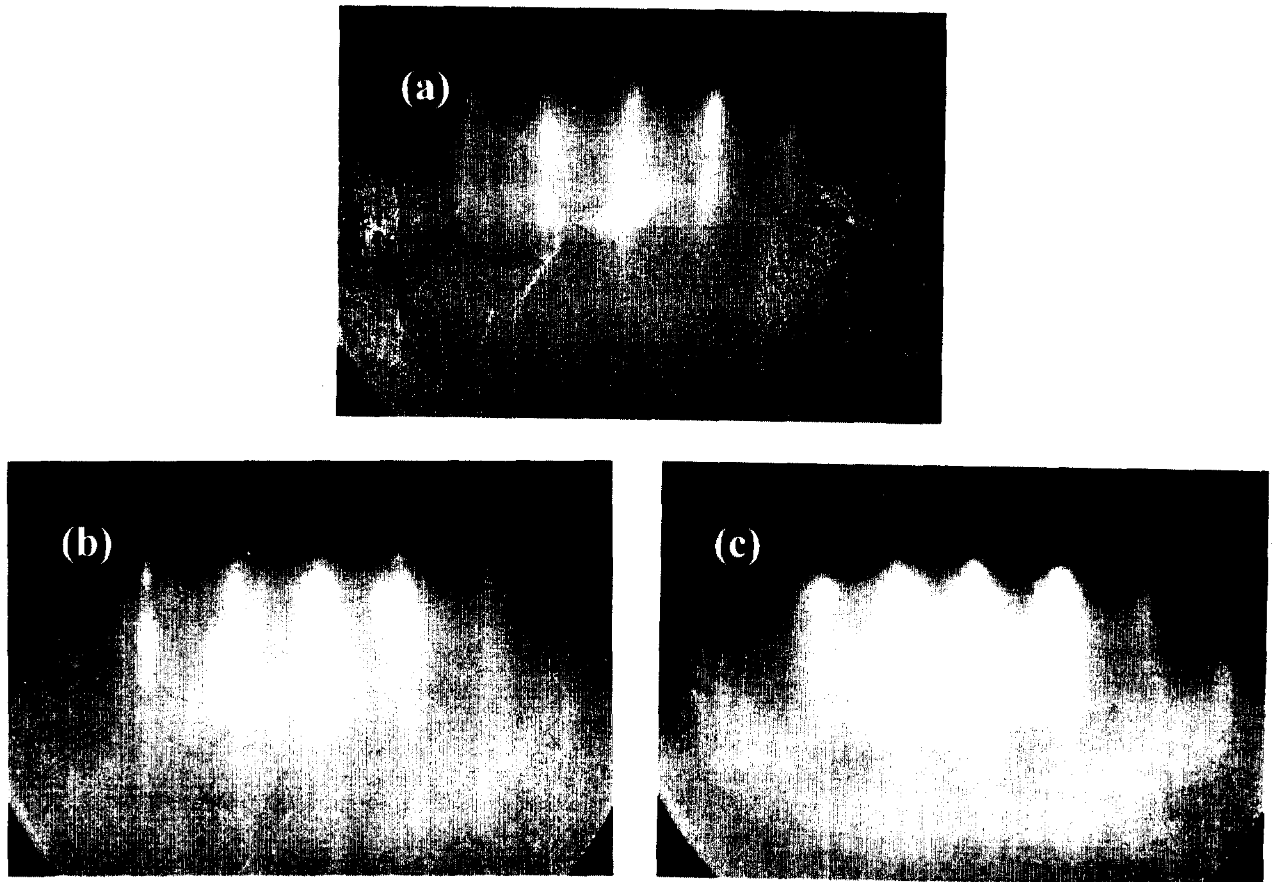


Figure 1. The RHEED patterns with the substrate temperature (a) 500 ℃, (b) 600 ℃, and (c) 700 ℃. The incident beam direction is along the [110] direction of the $Y_2O_3$ film and the acceleration voltage is 30 keV.

the surface region. Increasing the substrate temperature up to the 700 ℃, however, the Xmin value was slightly decreased to the 0.19 at the surface region. This result indicated that the improvement of the film crystallinity was mostly accomplished in the substrate temperature range of 500 ℃ to 600 ℃, not in the range of 600 ℃ to 700 ℃, as shown in the result of RHEED observation. However, the interface crystallinity in both cases of the substrate temperature of 600 ℃ and 700 ℃ was worse than the surface region. The Xmin values of the interface region were 0.39 and 0.26 at the substrate temperature of 600 ℃ and 700 ℃, respectively. In general, the defects owing to the lattice mismatch can result in the lower crystallinity at the interface region. If only the lattice mismatch was the cause of the poor

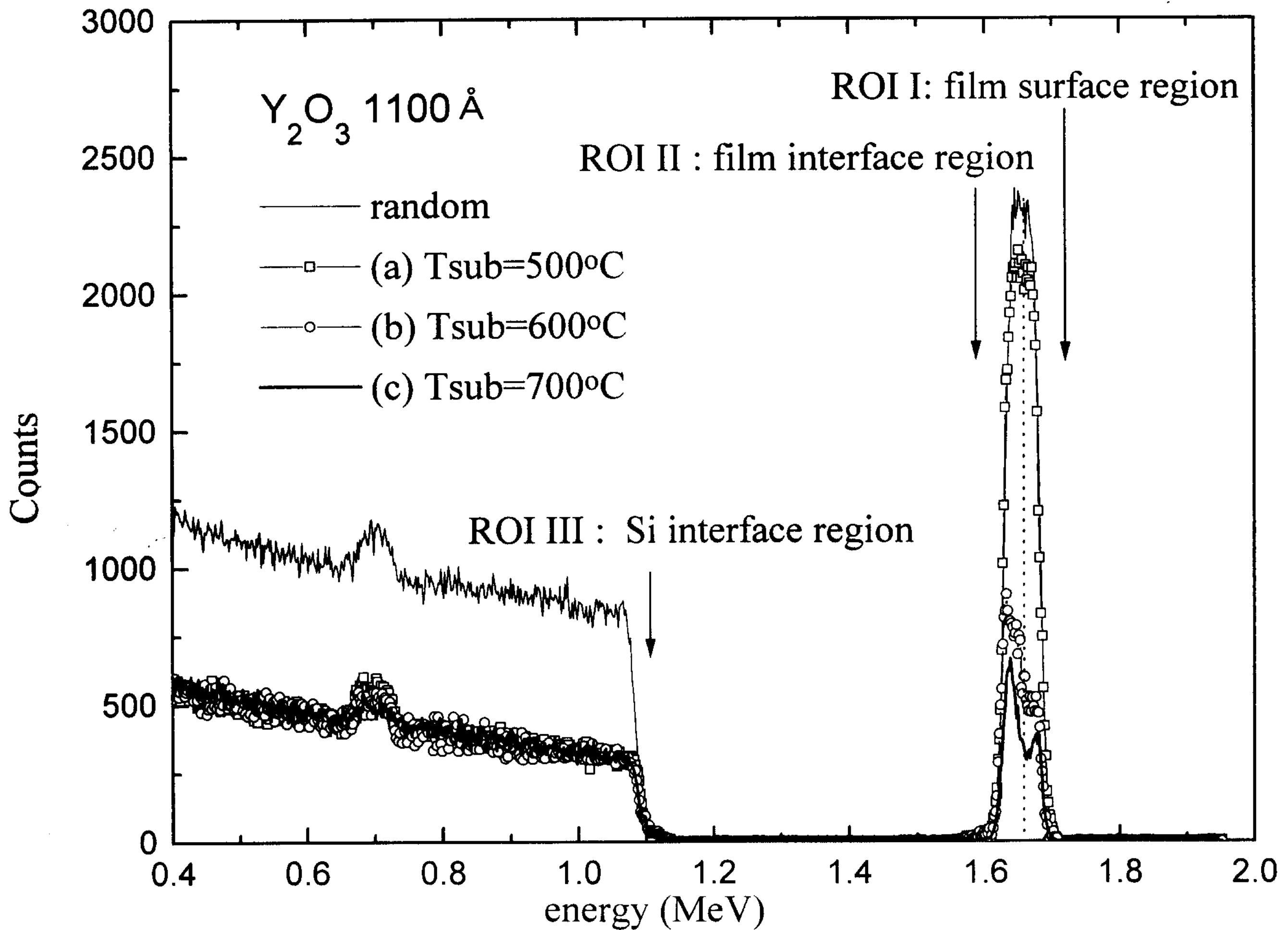


Figure 2. RBS/channeling spectra of the $Y_2O_3$ films grown at the substrate temperature of (a) 500 ℃, (b) 600 ℃, and (c) 700 ℃. All of the films have the thickness of 1100 Å. The detector angle is 170° with respect to the direction of the 2 MeV $He^{++}$ incident and nominal detector energy resolution is 14 keV.

interface crystallinity, however, the channeling yield difference between the interface region and surface was somewhat large. the poor crystallinity at the interface region was observed in the $CeO_2$/Si system, and the reason has been thought that the existence of high-density stacking faults due to the formation of the silicon oxide layer at the initial growth stage increased the channeling yield [4, 23]. If the silicon oxide layer was grown at the initial growth stage in this $Y_2O_3$/Si system, the thickness of the layer would be increased as the substrate temperature increased, so that the nucleation of the $Y_2O_3$ film would be disturbed by the silicon oxide layer. Therefore, the channeling yield would not be decreased. However, the crystallinity at the interface region was improved as the substrate temperature increased. Moreover, the further

decrease of the Xmin value at the interface region was generated. That is, the change of the crystallinity at the interface region was larger than that at the surface region, when the substrate temperature increased from 600 ℃ to 700 ℃. This indicated that the interface region could not have amorphous silicon oxide layer. In order to investigate the interface region, the HR-TEM was used. The image of the $Y_2O_3$ film clearly showed that the interface region did not have any inter layer oxide, and the boundary between the substrate and film was sharp as shown in the figure 3. Therefore, as we conjectured from the RBS channeling results, the poor interface crstallinity did not come from the silicon oxide layer. This result would be owing to the ion beam characteristic such as the weak sputtering and to the chemical reaction between the substrate and film. The accelerated ion beam can sputter the thin silicon oxide layer formed by the oxygen adsorption at the initial growth stage, and the metal yttrium can react not only with the silicon under the low oxygen partial pressure but also with oxygen under the high oxygen partial pressure [24-26]. This reaction can determine the film characteristics at the

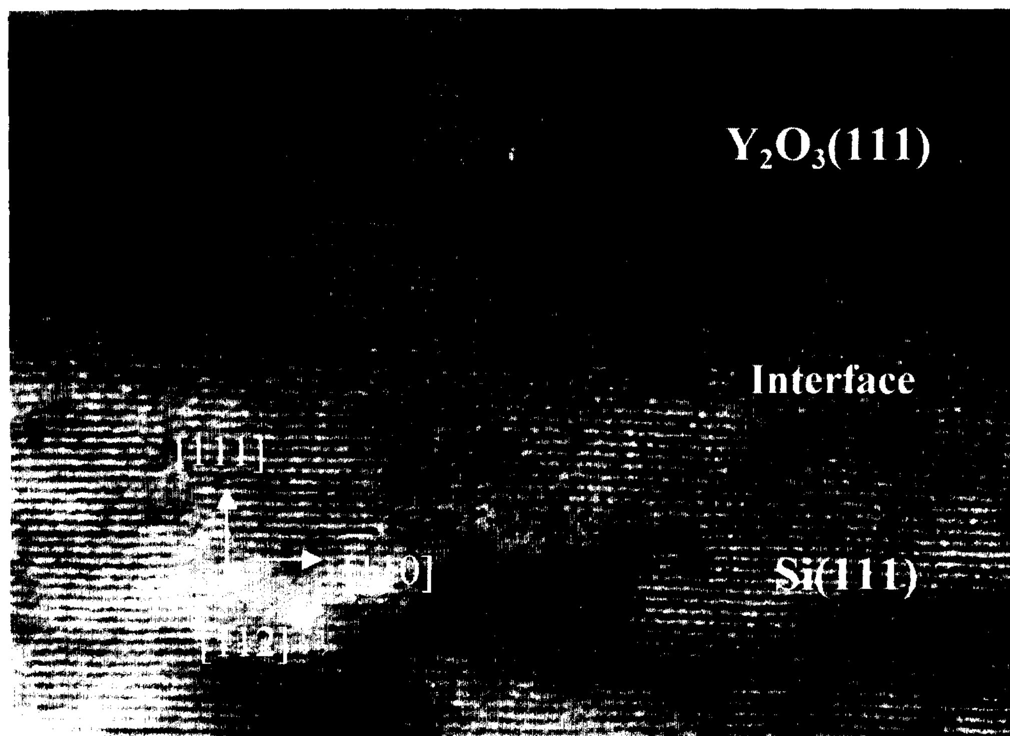


Figure 3. HR-TEM image of $Y_2O_3$(111)/Si(111). The film was grown at the substrate temperature of 600 ℃ and ion acceleration voltage of 5 kV. The interface region does not have any inter layer oxide and the boundary between the substrate and film is sharp.

initial growth stage.

We noticed that the improvement of the crystallinity mostly happened at the limiting range of the substrate temperature 500 ℃ to 600 ℃. Therefore, it can be inferred that the energy supplied by substrate temperature in the range of 600 ℃ and 700 ℃ will be dominantly used for another film characteristic, instead of improving crystallinity. When the substrate temperature increases, the reaction forming the yttrium silicide or the silicon oxide layer on the Si substrate surface is active, so that the formation of $Y_2O_3$ film is disturbed at the initial growth stage. The transformation of substrate surface state owing to the reaction influences not only the crystallinity but also interface stress. Therefore, the stress and crystallinity relation with the substrate temperature can present more information on the origin which influences the film quality.

B. Stress effect.

The stress of a film affects its performance and also reveals information on the behavior of the deposition process. The stress of heteroepitaxial films was investigated by two methods through the shift of x-ray rocking curve and of the channeling yield profile. The change of the strain with the substrate temperature were explored in figure 4, in which rocking curve scans of films grown on Si(111) substrates are shown. These curves presented the information of the temperature dependence on the crystallinity and strain. The change of the FWHM with the substrate temperature indicated that the crystallinity was improved as shown in figure 4 (b). The change of lattice constant from the rocking curve shift illustrated that the film was forced by compressive stress as the substrate temperature increased. In the temperature range of 600 ℃ to 700 ℃, the increment of the lattice constant was relatively larger than that in the range of 500 ℃ to 600 ℃. This characteristic and the channeling data from figure 2 presented the information on the behavior of the deposition process. The supplied energy from the temperature range of 600 ℃ to 700 ℃ was dominantly used to increase the

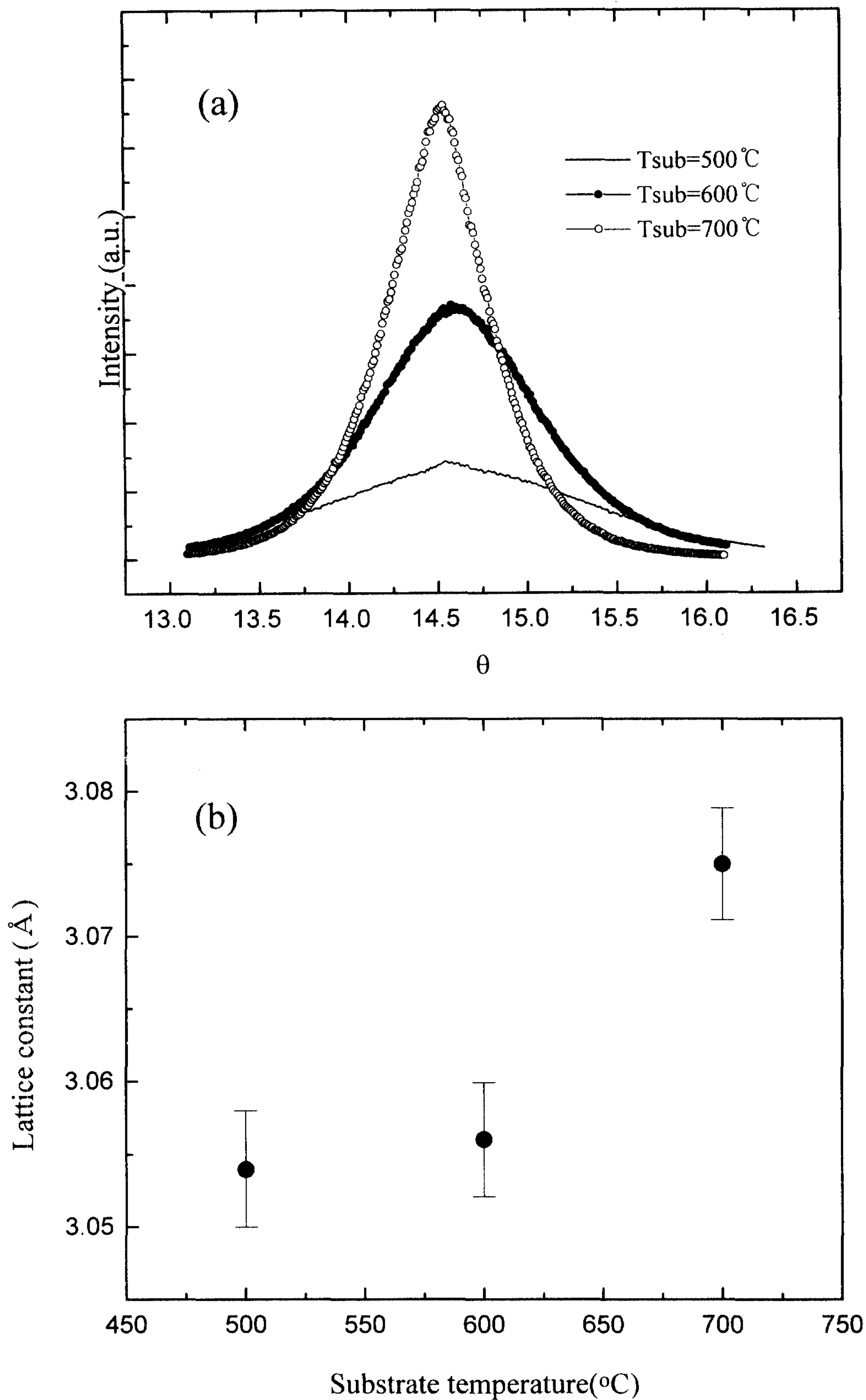


Figure 4. (a) X-ray rocking curves of the $Y_2O_3$ films grown at the substrate temperature of 500 ℃, 600 ℃, and 700 ℃. (b) The change of lattice constant and FWHM from the rocking curve with the substrate temperature.

compressive stress, while the energy from the substrate temperature in the range of 500 ℃ to 600 ℃ was mainly used to improve the crystallinity as the reduction of the disorder. The further increment of the lattice constant in the substrate temperature range of 600 ℃ to 700 ℃ can be thought that the thermal expansion coefficient of the film ($\alpha_f$=8×10$^{-6}$ Cm/℃) relative to the substrate ($\alpha_s$=3.8×10$^{-6}$ Cm/℃), the grain growth, and film density brought the increase of the compressive stress. In order to find out which effect influenced the compressive stress with the substrate temperature, the refractive index was investigated using the ellipsometery. Increasing the substrate temperature, the coefficient increased and approached the value in bulk $Y_2O_3$ ($n_f$=1.915) as shown in figure 5. According to the further increment of the index between the substrate temperature of 600 ℃ and 700 ℃, we inferred that the stress effect resulted from the film density. This effect will be again considered by investigation of surface morphology in subsection C.

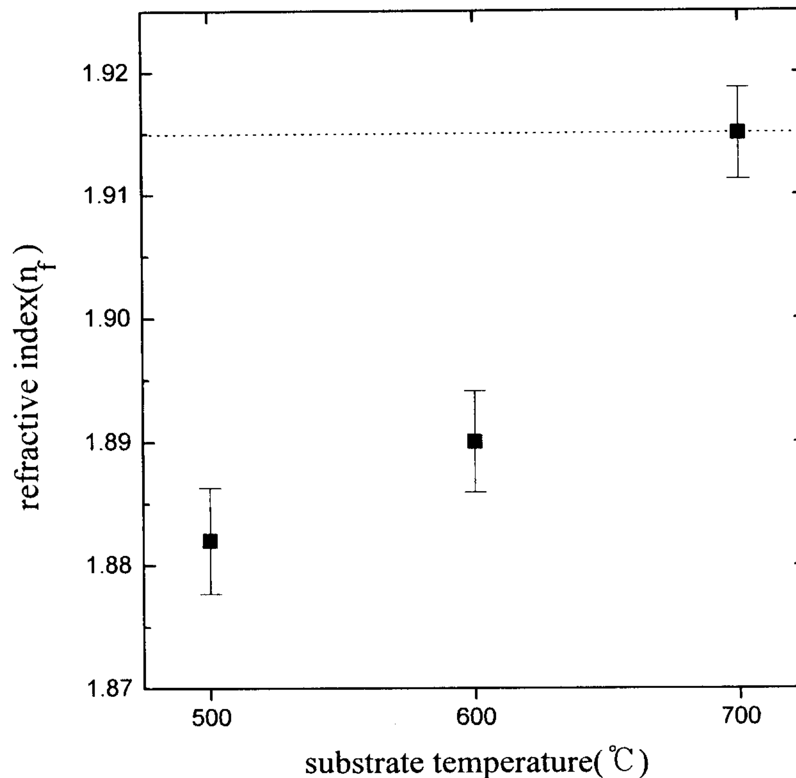


Figure 5. Refractive index $n_f$ of 1100 Å $Y_2O_3$ thin films deposited by ICB at different substrate temperature.

Using an ion channeling method, the strain can be measured through the deviation $\Delta\psi$ in the angle between the minimum channeling yield expected for the cubic system and that found in the strained system. Figure 6 showed the change of the channeling yield of $Y_2O_3(111)$ grown at the substrate temperature of 600 ℃ with channeling angular scan. The normalized yields in the three regions, film surface region(ROI I), film interface(ROI II), and substrate interface(ROI III) as marking in figure 2 were 0.26, 0.39, and 0.45, respectively. While the positions with the minimized yield in the film surface region had the same position in substrate interface region, the position in the film interface region did not accord with that of the substrate interface region; i.e., the deviation $\Delta\psi$ was about 0.1° between the substrate interface region and the film interface region. This illustrated that the strain in the film existed in the interface region, not in the film surface region. In YSZ growing in Si, the deviation about 0.45° due to the interface $SiO_2$ layer existed [27]. However, the deviation in $Y_2O_3$ film was very small compared with the value in the YSZ film, and the interface oxide layer did not exist in this $Y_2O_3$/Si system as shown in HR-TEM image of figure 3. Therefore, the deviation does not result from the oxide layer. According to the suppression of silicon oxide layer at the interface, it can be inferred that the transformation of the substrate surface came from the interface reaction between the metal yttrium and $SiO_2$ layer formed at the initial growth stage, and induced the interface strain. In particular, using the ion beam of yttrium, this reaction can be affected by the energetic beam. The impact of ion beam influences the reaction mechanism between yttrium and oxygen or between yttrium and silicon. Therefore, we can consider two different reaction system at initial growth stage. First, the shallowly implanted yttrium can react easily with silicon, not with oxygen, and yttrium silicide formation can occur. The crystallinity of the $Y_2O_3$ is disturbed by the formation of yttirum silicide layer, and many defects are generated at interface region [28-29]. As the substrate temperature is increased, the generation of the defects in the film at initial growth stage is decreased, so that

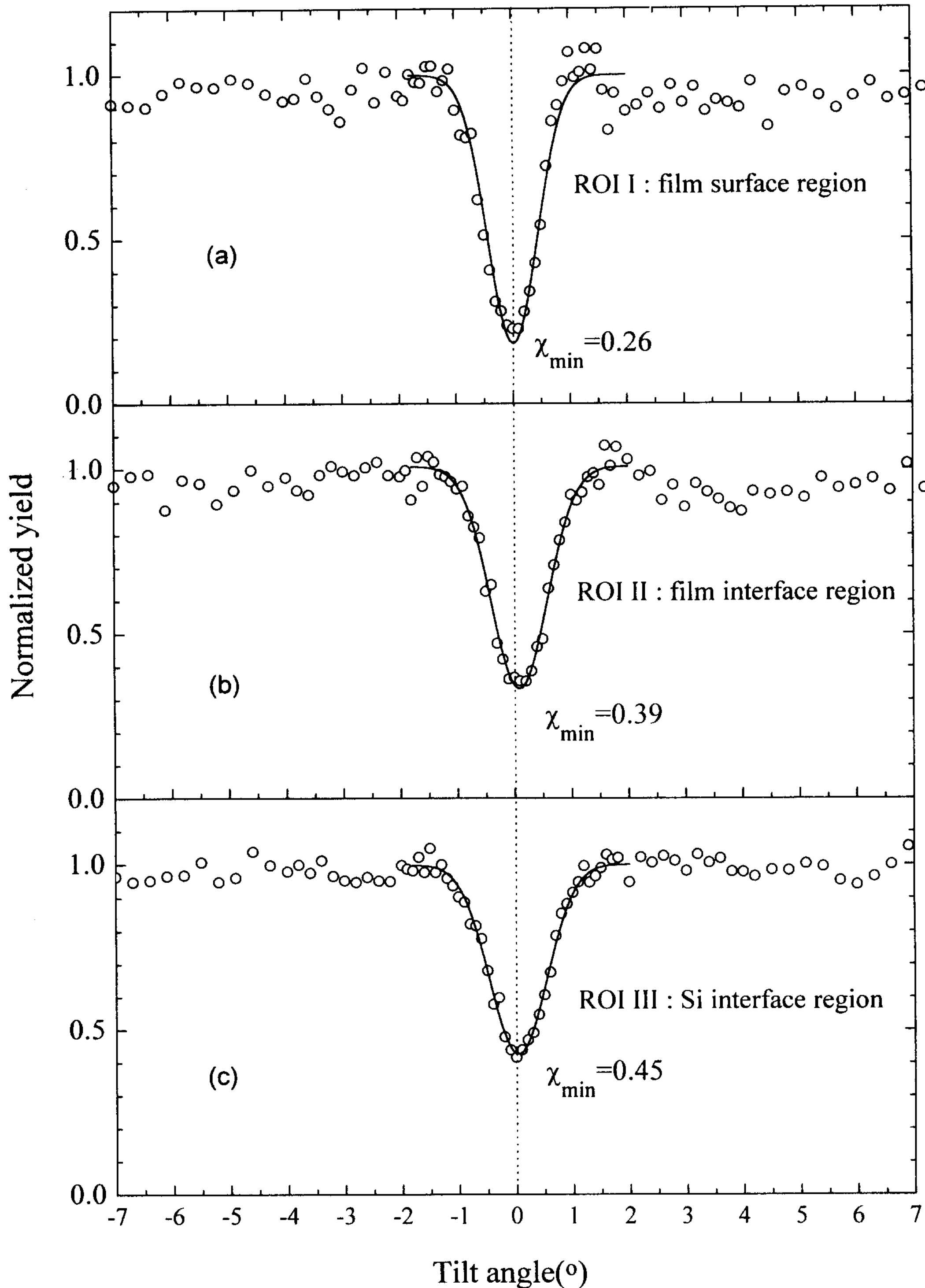


Figure 6. RBS/channeling yields for $Y_2O_3$ films epitaxially grown on Si(111) at the substrate temperature of 600 ℃. The yields were taken at the different three regions, film surface region (ROI I), film interface region (ROI II), substrate interface region (ROI III) in order to get information on the crystallinity and strain with respect to the depth direction of the film.

the improvement of the crystllinity at the interface is higher than that at the surface region. Also, the high density film can be obtained. Therefore, the Y2O3 film with the high crystallinity and density, and the interface silicide layer can block the diffusion of oxygen across the film layer. Second, yttrium can react with the oxygen in $SiO_2$ layer which formed at initial growth stage [19]. The $SiO_2$ layer will be consumed by reaction with yttrium, and $Y_2O_3$ layer will be formed. However, many defects will be generated at the interface, because the formation of $Y_2O_3$ at that time requires an additive energy to break the bond between silicon and oxygen. The defects degenerate the interface crystallinity and influence the interface stress. We can not determine which reaction can dominantly influence the interface characteristic. However, in the TEM image, since the many defects were found and any inter-layer oxide did not exist at interface, it is reasonable that the generation of the defects due to the reactions is the reason for the low interface crystallinity and strain at interface region.

C. Surface and interface roughness

The variation of the morphological shape at the surface and interface regions are related with the above two effect, so that the usual information can be presented by investigation of the shape variation. The film surface and interface roughness were investigated by AFM and x-ray scattering, respectively. The figure 7 showed the AFM images of the films grown at the substrate temperature of (a) 500 ℃, (b) 600 ℃, and (c) 700 ℃, respectively. The morphological shape was transformed from elliptical shape to triangular, and the grain size was gradually decreased. While the shape transformation was observed in the temperature range of 600 ℃ to 700 ℃ as shown in figure 7 (b) and 7 (c), the decrease of roughness changed drastically in the temperature range of 500 ℃ to 600 ℃ as illustrated in figure 6 (d). In the previous section, we observed that the crystallinity improved particulary in the temperature range of 500 ℃ to 600 ℃, and the film strain occurred dominantly in the temperature range of

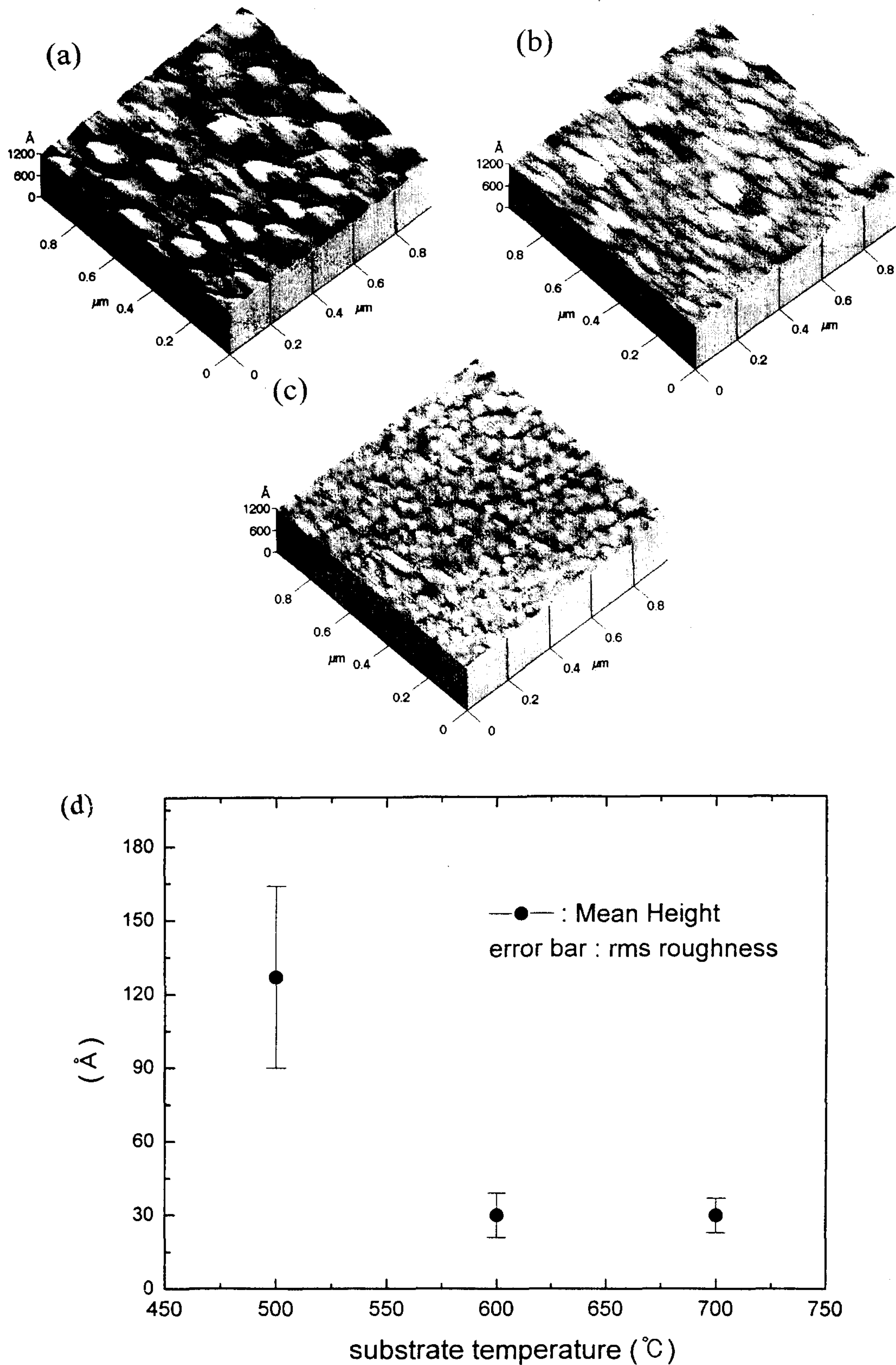


Figure 7. AFM images of the surface morphology of 1100 Å $Y_2O_3$ films grown under different substrate temperature. (a) Substrate temperature 500 ℃. (b) Substrate temperature 600 ℃. (c) Substrate temperature 700 ℃. (d) rms roughness change with the substrate temperature by AFM data.

600 ℃ to 700 ℃. Therefore, the change of surface roughness can closely relate with the crystallinity, and the morphological shape transformation relate with the film strain. The surface roughness can provide the information of the surface migration, because the surface migration energy can increase the surface flatness. Therefore, the decrease of surface roughness simultaneously improves the crystallinity. The sufficiently provided energy to the deposited atoms can give the increase of surface migration. As a result, the atoms migrate into the position with the overall minimized energy, so that the film density is increased. The AFM image showed the increase of the grain density and the decrease of the grain size with the substrate temperature. Therefore, it seemed that the grain density was the main factor of the compressive stress as shown in the result of refractive index These results were well consistent with the previous results by RBS channeling, XRD, and ellipsometery. In general, the increase of the grain size makes the film density increase. However, our result shows that the grain size decreased, although the film density increased. This tendency comes from the transformation of the substrate surface due to the interface reaction and the ion beam characteristic.

The film surface characteristic such as morphology and roughness can be qualitatively well investigated by AFM. However, the film interface properties can not be explored by AFM. We used the x-ray scattering method to observe the interface roughness characteristics. As shown in figure 8, the specula reflectivity measured on the 500 Å $Y_2O_3$ film grown at the substrate temperature of 600 ℃ and 700 ℃. The data were taken along the $q_z$ direction keeping the in-plane momentum transfer fixed to zero, $q_x$=$q_y$=0. The regular intensity oscillations resulted from the nature of the $Y_2O_3$ film thickness, and indicated that the film was quite uniform in thickness. The decay of the overall intensity and the amplitude of the oscillations in the specula-reflectivity curve provide crucial information on the roughness of both the air/ $Y_2O_3$ and $Y_2O_3$/Si interfaces. The roughness of each interface contributes to the

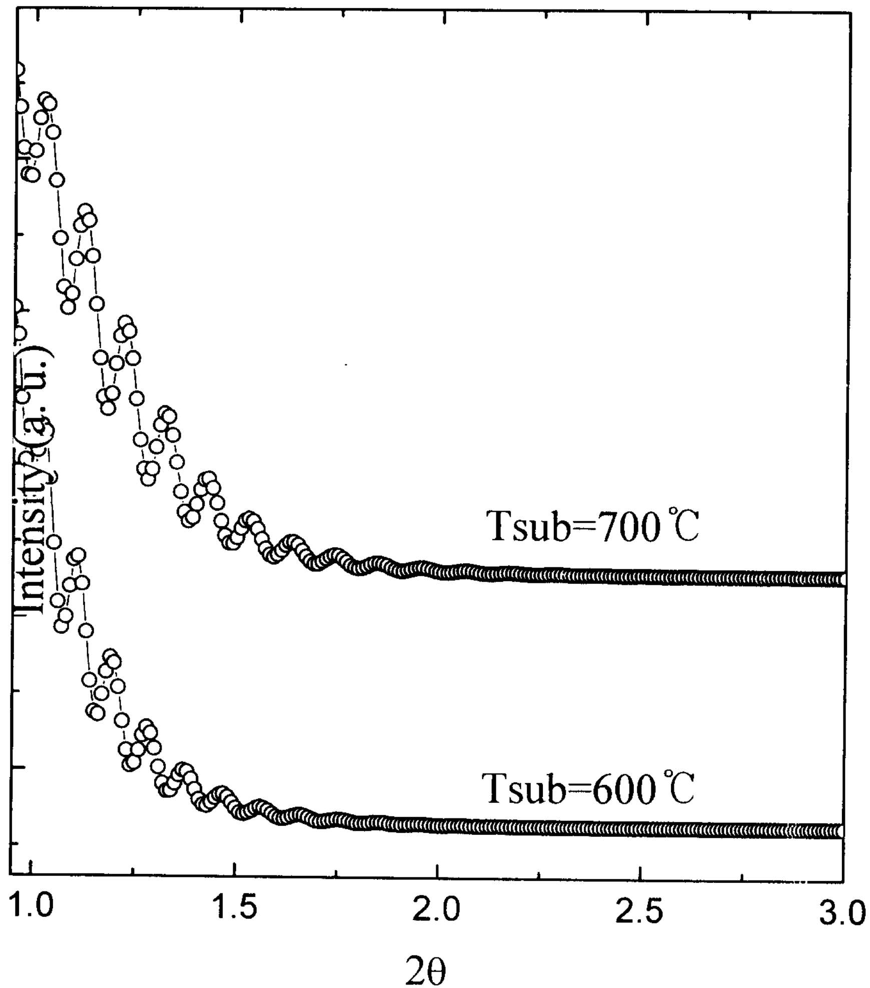


Figure 8. The x-ray reflectivity data obtained on the 500 Å $Y_2O_3$ film grown under different substrate temperature of 600 ℃ and 700 ℃. The intensity oscillations were originated from the interference between the film surface and the film-substrate interface.

overall decay of the reflectivity. The surface roughness was about 10 Å and 7 Å, and the interface roughness was about 17 Å and 12 Å at the substrate temperature of 600 ℃ and 700 ℃, respectively. Increasing the substrate temperature, the surface and interface roughness were all decreased, and the interface region was rougher than the surface region. Also, the decrease of interface roughness was larger than that of surface region. This result was well matched with crystallinity result of the RBS channeling data. Therefore, the film with rougher interface had worse crystallinity. Therefore, we can conclude that the surface transformation by the reaction or the ion beam characteristic by shallow implantation induced rougher interface which included many defects.

## IV. CONCLUSIONS

We investigated the temperature dependence of the crystallinty, strain, and morphological characteristics of the epitaxial $Y_2O_3$ films grown on Si(111) by reactive ICB.
Each characteristic has temperature dependence on the limiting temperature range; i.e., in the temperature range of 500 ℃ to 600 ℃, the crystallintiy was dominantly improved, and the surface roughness was drastically decreased. On the other hand, in the temperature range of 600 ℃ to 700 ℃, the film was more compressed, and the density was mainly increased. Also, the morphological shape was transformed from the elliptical shape to triangular. The crystallintiy and the roughness at the interface region was worse than that at the surface region, so that the film stress existed dominantly at the interface region.

According to the interface characteristics from the RBS channeling data, TEM image, and x-ray reflection, it can be inferred that many defects at the interface region were generated by the interface reaction between the yttrium and $SiO_2$ layer and by the impact of yttrium ion beam. The surface transformation by defects generation influences the film qualities such as the crystallinity, stress and morphology. Therefore, the defect control, that is, interface reaction control is the main factor in order to increase the film crystallinity.

## REFERENCES


1. D. K. Fork, D. B. Fenner, G. A. Connell, Julia M. Phillips, and T. H. Gabelle, Appl. Phys. Lett., **57(11)**, 1137 (1990).

2. A. Lubig, Ch. Buchal, D. Guggi, C. L. Jia, and B. Stritzker, Thin Solid Films, **217**, 125 (1992).

3. M. Morita, H. Fukumoto, T. Imura, Y. Osaka, and M. Ichihara, J. Appl. Phys. 58(6), **2407** (1985)

4. T. Inoue, Y. Yamamoto, S. Koyama, S. Suzuki, and Y. Ueda, Appl. Phys. Lett., **56(14)**, 1332 (1990)

5. D. K. Fork, D. B. Fenner, and T. H. Geballe, J. Appl. Phys., **68(8)**, 4316 (1990)

6. A. Bardel, O. Eibl, Th. Matthee, G. Friedl, and J. Wecker. J. Mater. Res. **8(9)**, 2112 (1993)

7. L. Manchanda and M. Gurvitch, IEEE electron device Lett., **9**, 180 (1988).

8. C. Hu: IEDM Technical Digest (IEEE, New York,1985) p.368.

9. A. C. Rastogi and R. N. Sharma, J. Appl. Phys., **71**, 5041 (1992).

10. David K. Fork, David B. Fenner, Adrian Barrera, Julia M. Phillips, Theodore H. Geballe, G. A. N. Connell and James B. Boyce, IEEE transaction on applied superconductivity, **1(1)**, 61 (1991).

11. Th. Matthee, J. Wecker, H. Behner, G. Friedl, O. Eible, and K. Samwer, Appl. Phys. Lett., **61(10)**, 1240 (1992).

12. M. Gurvitch, L. Manchanda, and J. M. Gibson, Appl. Phys. Lett., **51**, 919 (1987).

13. H. Fukumoto, T. Imura and Y. Osaka, Appl. Phys. Lett., **55**, 360 (1989).

14. K. Harada, H. Nakanishi, H. Itozaki and S. Yazu, Jpn. J. Appl. Phys., **60**, 934 (1991).

15. A. F. Jankowski, L. R. Schrawyer, and J. P. Hayer, J. Vac. Sci. Technol., **A11**, 1548 (1993).

16. W. M. Cranton, D. M. Spink, R. Stevens, and C. B. Thomas, Thin Solid Films, **226**, 150

(1993).

17. R. W. Tustison, T. E. Varitimos, D. G. Montanari, and J. M. Wahl., J. Vac. Soc. Technol. **A7(3)**, 2256 (1989).

18. H. M. Choi, and S. K. Choi, J. Vac. Soc. Technol. **A13(6)**, 2832 (1995).

19. S. C. Choi, M. H. Cho, S. W. Whangbo, and C. N. Whang, Appl. Phys. Lett., **71(7)**, 903 (1997).

20. K. W. Kim, S. C. Choi, S. S. Kim, S. J. Cho and C. N. Whang, J. Mater. Sci., **28**, 1537 (1993).

21. S. J. Cho, H. S. Choe, S. C. Choi, K. W. Kim, H. K. Jang, S. S. Kim, and C. N. Whang, Nucl. Instrum. Methods., **B 59/60**, 1247 (1991).

22. K. W. Kim, C. E. Hong, S. C. Choi, S. J. Cho, C. N. Whang, T. E. Shim and D. H. Lee, J. Vac. Sci. Technol., **A12**, 3180 (1994).

23. R. G. Schwab, R. A. Steiner, G. Mages, and H. -J. Beie, Thin Solid Films, **207**, 283 (1992).

24. T. L. Lee, and L. J. Chen, J. Appl. Phys., **73(12)**, 8258 (1993).

25. Susumu Horita, Yukinari Abe, and Tsuyoshi Kawada, Thin Solid Films, **281/282**, 28 (1996).

26. M. Gurivitch, L. Manchanda, and J. M. Gibson, Appl. Phys. Lett., **51(12)**, 919 (1987).

27. Hirofumi Fukumoto, Masateru Yamamoto, Yukio Osaka, and Fumitaki Nishyama, J. Appl. Phys., **67(5)**, 2447 (1990)

28. J. A. Knapp and S. T. Picraux, Appl. Phys. Lett. **48(7)**, 466 (1986).

29. Michael P. Siegal, William R.Graham, and Jorge J. Santigo-Vviles, J. Appl. Phys., **68(2)**, 574 (1990).